

# Simultaneous Detection of Dual Prostate Specific Antigens Using Surface-Enhanced Raman Scattering-Based Immunoassay for Accurate Diagnosis of Prostate Cancer

Ziyi Cheng,<sup>†</sup> Namhyun Choi,<sup>†</sup> Rui Wang,<sup>†</sup> Sangyeop Lee,<sup>†</sup> Kyung Chul Moon,<sup>‡</sup> Soo-Young Yoon,<sup>‡</sup> Lingxin Chen,<sup>\*,§</sup> and Jaebum Choo<sup>\*,†</sup>

<sup>†</sup>Department of Bionano Technology, Hanyang University, Ansan 426-791, South Korea

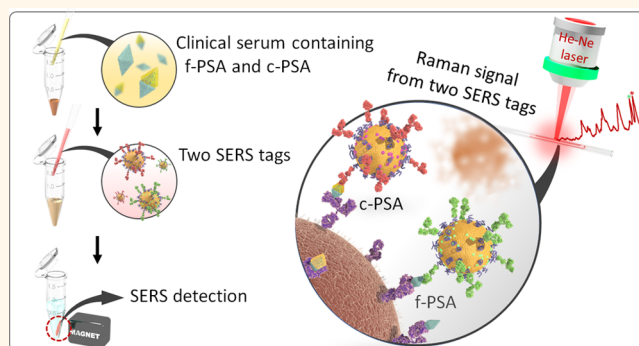
<sup>‡</sup>Department of Laboratory Medicine, Korea University College of Medicine, Seoul 152-854, South Korea

<sup>§</sup>Key Laboratory of Coastal Environmental Processes and Ecological Remediation, Yantai Institute of Coastal Zone Research, Chinese Academy of Sciences, Yantai, Shandong 264003, China

## Supporting Information

**ABSTRACT:** Accurate analysis of specific biomarkers in clinical serum is essential for early diagnosis and treatment of cancer. Here, a surface-enhanced Raman scattering (SERS)-based immunoassay, using magnetic beads and SERS nano tags, was developed for the determination of free to total (f/t) prostate specific antigen (PSA) ratio to improve the diagnostic performance of prostate cancer. To assess the clinical applicability of the proposed method, SERS-based assays for the simultaneous detection of dual PSA markers, free PSA (f-PSA) and complexed PSA (c-PSA), were performed for clinical samples in the gray zone between 4.0 and 10.0 ng/mL. Our assay results for f/t PSA ratio showed a good linear correlation with those measured using the electrochemiluminescence (ECL) system installed in the clinical laboratory of the University Hospital. In addition, the simultaneous assay provided better precision than parallel assays for the detection of f-PSA and c-PSA in 13 clinical serum samples. Therefore, our SERS-based assay for simultaneous detection of dual PSA markers in clinical fluids has strong potential for application in the accurate diagnosis of prostate cancer.

**KEYWORDS:** SERS-based immunoassay, multiplex detection, prostate cancer, free to total PSA ratio, simultaneous detection



Prostate cancer is the second leading cause of cancer death in the United States. The most commonly used test for prostate cancer is a prostate specific antigen (PSA) test, that measures the level of total PSA (t-PSA) in blood serum.<sup>1</sup> However, it is known that the PSA blood test is not specific for prostate cancer because t-PSA can be increased due to other factors including benign prostatic hyperplasia (BPH) or prostatitis as well as prostate cancer.<sup>2,3</sup> Thus, medical doctors cannot make a final decision of whether a man has life-threatening prostate cancer based only on an elevated level of t-PSA. Consequently, t-PSA testing alone is not sufficient to accurately diagnose prostate cancer.<sup>4</sup> Most of the PSA protein released into the bloodstream is attached to other blood proteins. Some of the PSA forms complexes with the serum protease inhibitor  $\alpha$ 1-antichymotrypsin to create a bound form called complexed PSA (c-PSA).<sup>5</sup> PSA that does not combined with other proteins is known as free PSA (f-PSA). It has been

reported that the level of f-PSA is decreased in men who have prostate cancer compared with those with benign conditions. Therefore, the free to total PSA ratio can be additionally used in clinical diagnostics to discriminate between prostate cancer and BPH.<sup>6–8</sup> This is particularly useful for patients with a t-PSA level that falls in the “diagnostic gray zone” between 4.0 and 10.0 ng/mL.<sup>9,10</sup> From a clinical point of view, higher t-PSA level and lower percentage of f-PSA are associated with a higher risk of prostate cancer.

Therefore, detection of both f-PSA and c-PSA in serum is crucial for the accurate diagnosis of prostate cancer. Various immunoassay technologies including enzyme-linked immuno-

Received: March 3, 2017

Accepted: April 25, 2017

Published: April 25, 2017

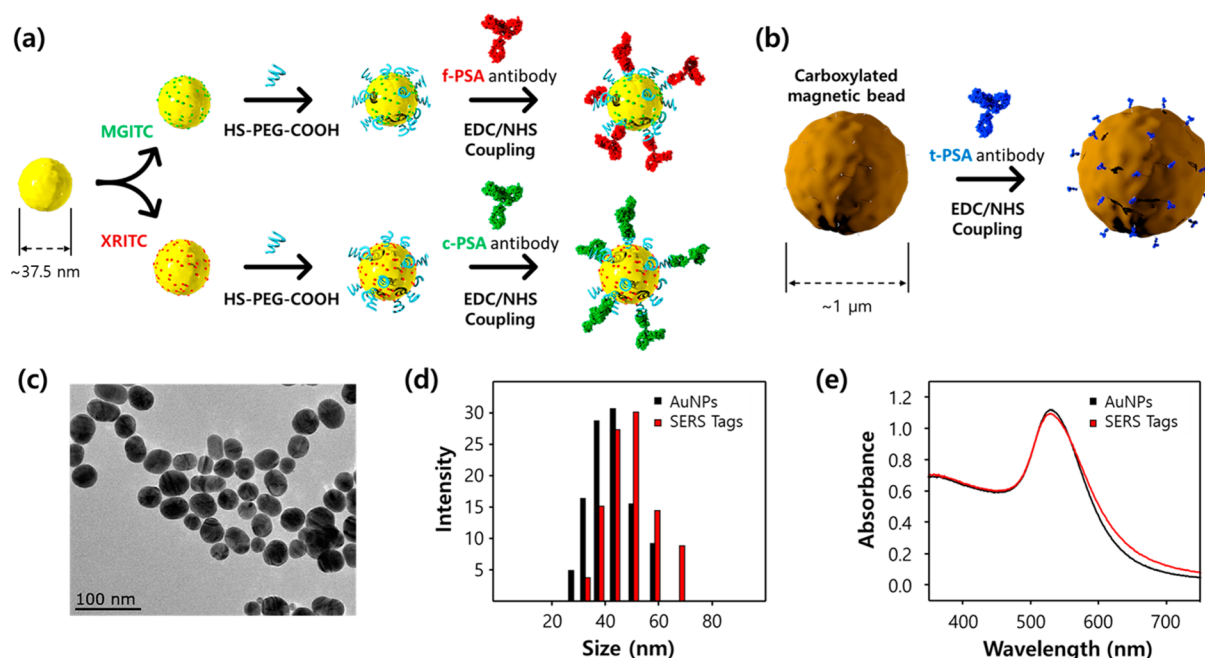


**Figure 1.** (a) Sequential process for fabricating two different types of antibody-conjugated SERS nano tags. (b) Antibody immobilization on the surface of a magnetic bead. (c) TEM image of SERS nano tags. (d) DLS distributions of AuNPs (black) and SERS nano tags (red). (e) UV-vis spectra for AuNPs (black) and SERS nano tags (red).

sorbent assay (ELISA),<sup>11</sup> fluorescence immunoassay,<sup>12</sup> surface plasmon resonance,<sup>13</sup> electrochemical immunosensor,<sup>14</sup> dark field microscopy,<sup>15</sup> chemiluminescence,<sup>16</sup> and dynamic light scattering<sup>17</sup> have been employed for the quantitative analysis of f-PSA and c-PSA. Through these techniques, however, detection of only a single biomarker per assay is possible, and two parallel immunoassay experiments must be performed for the estimation of both PSA levels.<sup>13,16</sup>

In recent years, a surface-enhanced Raman scattering (SERS)-based immunoassay technique using functional metal nanoparticles has attracted much interest due to its high sensitivity and multiplex detection capability.<sup>19–23</sup> When Raman reporter molecules adsorbed on nanoparticle surfaces are exposed to a single excitation light source, the incident light field is significantly enhanced at SERS active sites known as electromagnetic “hot junctions” by localized surface plasmon effects.<sup>24,25</sup> This enhancement effect has overcome the problems of low sensitivity inherent to conventional fluorescence or luminescence-based assay techniques.<sup>26–28</sup> Moreover, simultaneous detection of multiple biomarkers is possible in Raman spectroscopy since Raman peaks are much narrower than fluorescence emission bands.<sup>29,30</sup> In the present study, simultaneous detection of f-PSA and c-PSA markers in blood serum was performed using a SERS-based immunoassay technique. As described above, determination of f-PSA/t-PSA ratio is important for accurate diagnosis of prostate cancer, especially for patients with a t-PSA level in the gray zone.<sup>9,10</sup> For this purpose, two different types of SERS nano tags, one for f-PSA and the other for c-PSA, were prepared, and then magnetic sandwich immunocomplexes were formed for both PSA markers. To assess the feasibility of our proposed assay technique as a clinical tool in prostate cancer diagnosis, the SERS-based assay results for 30 clinical samples were compared with those measured by electrochemiluminescence (ECL) assay. In particular, we focused on the detection consistency between the methods especially for the 13 clinical samples in

which the t-PSA level was in the diagnostic gray zone. Some of the methods referenced have been multiplexed<sup>13,16</sup> but are not real simultaneous detection of both PSA markers. In the present work, however, simultaneous detection of dual PSA markers in blood serum was achieved using SERS-based assays under single wavelength excitation. It provides advantages over conventional methods, such as reduced sample consumption, rapid detection time, high detection throughput, and low cost per assay.<sup>6,18</sup> We expect that this approach will provide another insight into the accurate diagnosis of prostate cancer.

## RESULTS AND DISCUSSION

Figure 1 shows the sequential process for fabricating two different types of antibody-conjugated SERS nano tags (detection probes) and t-PSA-conjugated magnetic beads (capture substrates) for the simultaneous detection of f-PSA and c-PSA. In Figure 1a, malachite green isothiocyanate (MGITC) and X-rhodamine-5-(and-6)-isothiocyanate (XRITC) (Raman reporter molecules) were respectively immobilized on the surfaces of gold nanoparticles (AuNPs). SH-PEG-COOH was used for the conjugation of antibodies. Finally, f-PSA and c-PSA antibodies were immobilized on the surfaces of AuNPs through 1-ethyl-3-(3-(dimethylamino)propyl) carbodiimide (EDC)/N-hydroxysuccinimide (NHS) coupling. Carboxylic acid-functionalized magnetic beads were used for the fabrication of capture substrates. The surfaces of the magnetic beads were activated by EDC and NHS, and then t-PSA antibodies were immobilized on their surfaces as shown in Figure 1b. These t-PSA antibodies capture both f-PSA and c-PSA antigens in blood serum through antibody–antigen reactions. Figure 1c shows a transmission electron microscopy (TEM) image of SERS nano tags. The diameter was estimated to be  $43 \pm 5$  nm. Dynamic light scattering (DLS) and UV-vis measurements were also performed to confirm the size distribution of AuNPs and antibody-conjugated SERS nano tags as shown in Figures 1d and e. The average diameter of

AuNPs increased from 43 to 52 nm after antibody conjugations according to the DLS data in Figure 1d. UV–vis spectral data also demonstrated that the surface plasmon band was slightly shifted from 530 to 531 nm upon antibody conjugation. Figure 2 displays the Raman spectra of f-PSA antibody/MGITC-

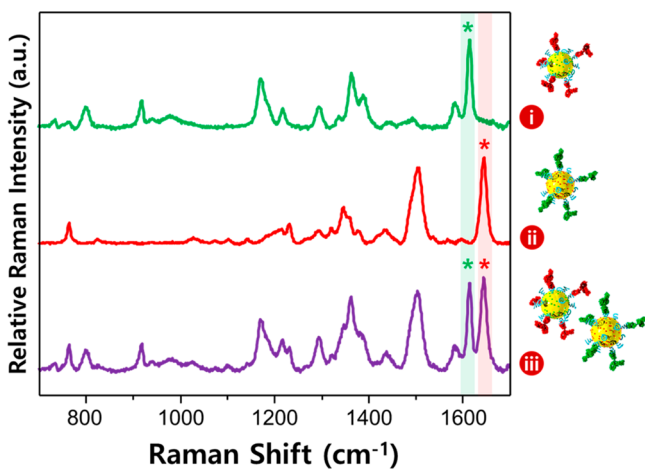


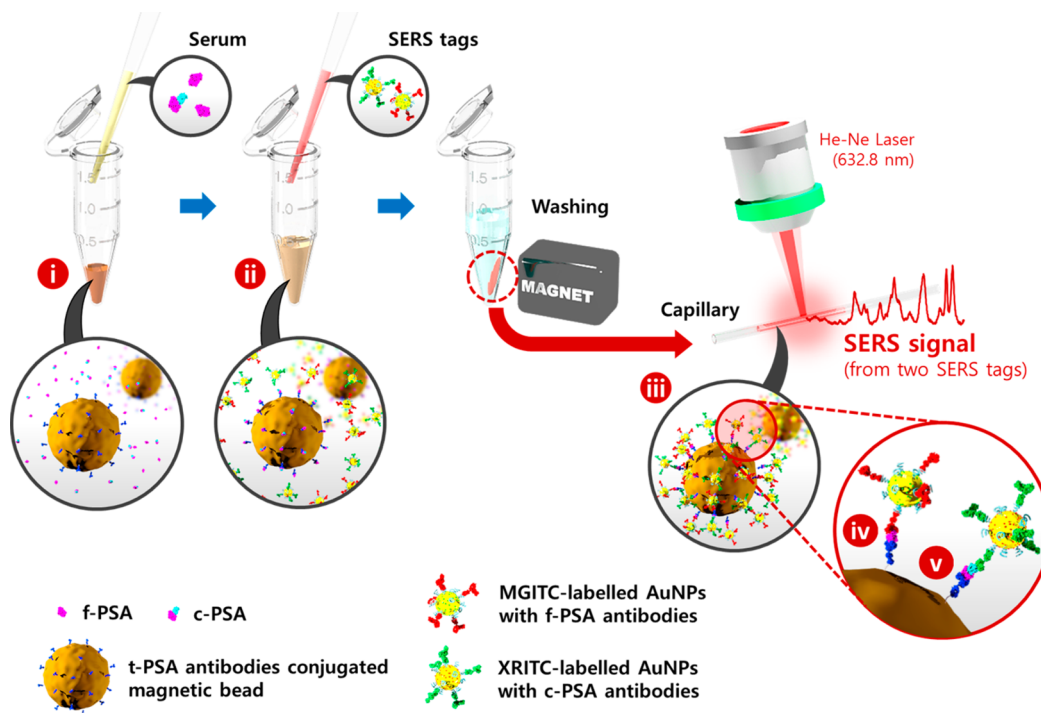
**Figure 2.** Raman spectra of (i) f-PSA antibody/MGITC-labeled AuNPs, (ii) c-PSA antibody/XRITC-labeled AuNPs and (iii) their 1:1 (V/V) mixture. Characteristic Raman peaks of MGITC ( $1614\text{ cm}^{-1}$ ) and XRITC ( $1646\text{ cm}^{-1}$ ) were used for quantitative evaluation of f-PSA and c-PSA markers in serum, respectively.

labeled AuNPs (green, (i), c-PSA antibody/XRITC-labeled AuNPs; red, (ii) and their 1:1 (v/v) mixture; purple, (iii)). Here, the characteristic Raman peaks of MGITC ( $1614\text{ cm}^{-1}$ ) and XRITC ( $1646\text{ cm}^{-1}$ ) were used for quantitative evaluation of f-PSA and c-PSA markers in serum, respectively because

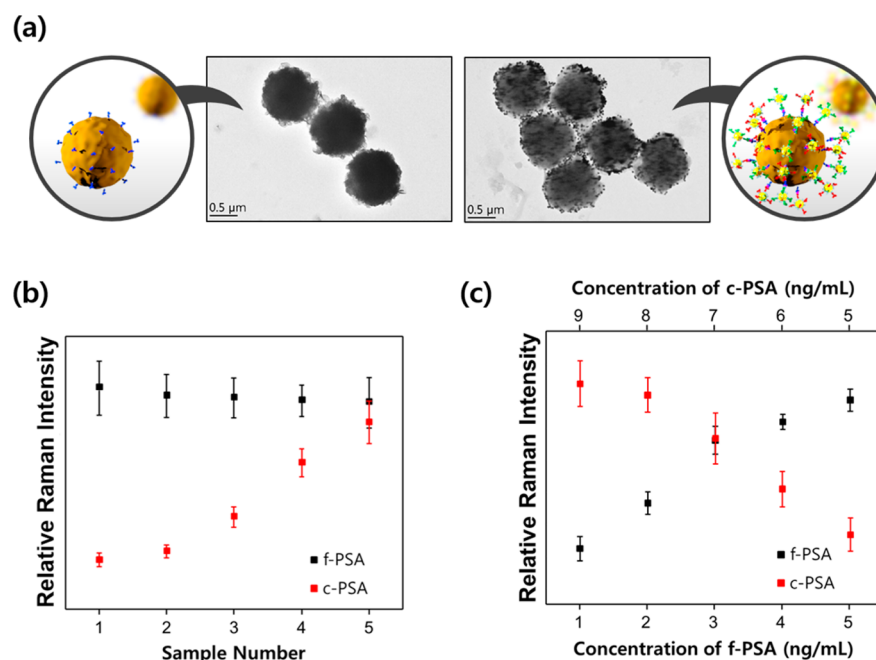
there is no overlap between the two peaks, as shown in the Raman spectrum for the mixture (iii).

Figure 3 illustrates the SERS-based assay process for the simultaneous detection of f-PSA and c-PSA. When a clinical serum containing f-PSA and c-PSA antigens was mixed with t-PSA-conjugated magnetic beads in a microtube, both antigens were captured on the surface of magnetic beads through antibody–antigen reactions. Next, f-PSA antibody/MGITC-labeled AuNPs (i) and c-PSA antibody/XRITC-labeled AuNPs (ii) were added to form sandwich immunocomplexes. These magnetic immunocomplexes were separated using a magnetic bar, and the Raman signals for each SERS nano tag were measured and analyzed for quantitative evaluation of f-PSA and c-PSA in blood serum. In this way, simultaneous detection of dual PSA markers could be achieved.

Minimum interference between two antibody/antigen sets is important for a multiplex immunoassay. To test the cross reactivity between f-PSA and c-PSA antigens, the concentration of f-PSA was kept constant at 10 ng/mL, whereas five different concentrations of c-PSA in the 1–10 ng/mL range were prepared and then two antigen solutions were mixed together. Each solution mixture was added to t-PSA antibody-conjugated magnetic beads and incubated for 30 min at room temperature. Finally, f-PSA and c-PSA SERS nano tags were added for formation of the two different types of immunocomplexes, and their Raman signals were measured. Figure 4a shows the corresponding Raman peak intensity changes for f-PSA and c-PSA. Here, the characteristic Raman peaks for MGITC ( $1614\text{ cm}^{-1}$ ) and XRITC ( $1646\text{ cm}^{-1}$ ) were used to monitor the quantity of each PSA antigen. The assay results indicate that the Raman intensity changes strongly depend on the concentration of f-PSA and c-PSA, and there was no serious cross reactivity between them because the Raman intensity for f-PSA (MGITC



**Figure 3.** Sequential SERS-based assay process for the simultaneous detection of f-PSA and c-PSA. (i) Mixing of f-PSA, c-PSA, and t-PSA antibody-conjugated magnetic beads. (ii) Addition of SERS nano tags to form sandwich immunocomplexes. (iii) Separation of magnetic immunocomplexes using a magnetic bar. Simultaneous detection of (iv) f-PSA and (v) c-PSA.



**Figure 4.** (a) TEM images of magnetic beads before and after the formation of magnetic immunocomplexes at a 5:5 molar ratio mixture of f-PSA and c-PSA. (b) Cross reactivity test for f-PSA and c-PSA antigens. The concentration of f-PSA was kept constant at 10 ng/mL with five different concentrations of c-PSA in the 1–10 ng/mL range. Raman peak intensity (MGITC at  $1614\text{ cm}^{-1}$ ) for f-PSA was constant regardless of c-PSA concentration, but the Raman intensity of XRITC at  $1646\text{ cm}^{-1}$  concomitantly increased with the increase in c-PSA concentration. (c) Raman intensity variations for different molar ratios of f-PSA and c-PSA (9:1, 8:2, 7:3, 6:4, and 5:5).

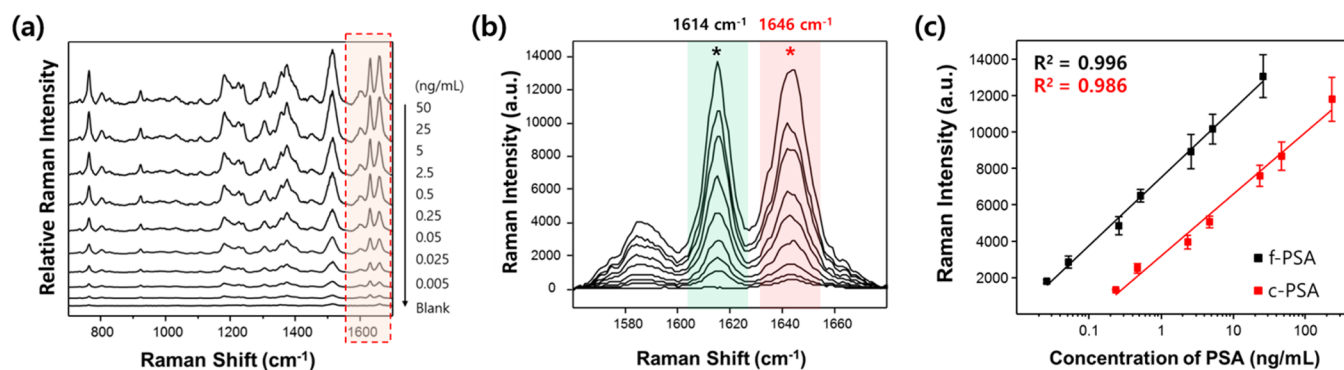


**Figure 5.** (a) Raman spectra for various concentrations of f-PSA and c-PSA spiked into human serum. Concentration ranges of f-PSA and c-PSA were 5.0 pg/mL–50 ng/mL and 45.0 pg/mL–450 ng/mL, respectively. (b) Raman peak intensity variations with increase in f-PSA and c-PSA concentrations in the  $1560\text{--}1680\text{ cm}^{-1}$  range. (c) Corresponding calibration curves for f-PSA and c-PSA. The error bars indicate standard deviations of five measurements.

at  $1614\text{ cm}^{-1}$ ) remained constant irrespective of f-PSA concentration, while the Raman intensity of XRITC at  $1646\text{ cm}^{-1}$  concomitantly increased with the increase of c-PSA concentration. Figure 4b also demonstrates the variations in Raman intensity for different molar ratios of f-PSA and c-PSA (9:1, 8:2, 7:3, 6:4, and 5:5). The results indicate that there is a linear correlation between the concentration of each PSA and corresponding Raman intensity. These data confirm that the proposed SERS-based assay can be used for quantitative evaluation of both PSA biomarkers. Figure 4c shows TEM images before and after formation of magnetic immunocomplexes (5:5 mixtures of f-PSA and c-PSA).

Before the simultaneous detection of f-PSA and c-PSA in clinical sera, we performed a SERS-based assay of t-PSA in 30 clinical samples collected from Korea University Medical Center in order to assess the clinical feasibility of our SERS-

based immunoassay. All clinical samples were handled in accordance with approved Institutional Review Board (IRB) protocols at the hospital. To obtain a standard calibration curve for t-PSA, various concentrations of t-PSA were spiked into commercially available steroid-free human serum. Raman signal intensity in the absence of t-PSA was used as a control. Figure S1a shows the Raman spectra of 12 different concentrations of t-PSA in commercial human serum. The concentration of t-PSA ranged from 0.001 to 200 ng/mL, and the characteristic Raman peak of MGITC at  $1614\text{ cm}^{-1}$  was monitored for construction of a calibration curve for t-PSA as shown in Figure S1b. The t-PSA concentration in real clinical serum samples was determined from this calibration curve. Our results of the SERS-based t-PSA assay for 30 clinical samples were compared with values measured using the COBAS ECL assay system installed at the clinical laboratory of the hospital (Table S1).

**Table 1.** Comparison of Free to Total PSA (f/t) Ratios between ECL- and SERS-based Assays for 13 Clinical Samples in the Gray Zone

sample no.	ECL assay <sup>a</sup>		SERS-based assay			
	t-PSA (ng/mL)	f/t PSA ratio	f/t PSA ratio (parallel assay)	f/t PSA ratio (simultaneous assay)	CV, % <sup>b</sup> (parallel assay)	CV, % <sup>b</sup> (simultaneous assay)
1	4.42	0.24	0.27	0.20	19.19	4.60
2	4.82	0.21	0.16	0.24	21.54	5.99
3	4.88	0.26	0.24	0.31	12.50	7.64
4	5.08	0.23	0.21	0.27	21.57	4.03
5	5.08	0.23	0.31	0.22	20.09	10.25
6	5.14	0.15	0.16	0.09	9.94	5.77
7	5.20	0.18	0.22	0.20	21.97	7.73
8	6.36	0.17	0.13	0.21	10.72	5.02
9	6.86	0.22	0.22	0.18	11.02	8.30
10	6.90	0.17	0.18	0.17	19.73	4.22
11	8.19	0.17	0.16	0.21	18.58	8.26
12	8.63	0.13	0.15	0.16	14.25	8.17
13	10.27	0.31	0.55	0.43	11.80	5.47

<sup>a</sup>Electrochemiluminescence. <sup>b</sup>Mean CVs were estimated to be 16.38 and 6.57 for parallel and simultaneous assays, respectively. All PSA concentrations are average values of five measurements.

The results of t-PSA measured from the SERS-based assay were consistent with those measured from the ECL system within the clinical acceptable range. Passing-Boblok regression analysis was performed to evaluate the similarity between SERS and ECL-based assay results. The plots in Figure S2 demonstrate a good agreement between the two analytical methods since the data points show a strong linear relationship.

As described in the Introduction Section, however, the t-PSA test is not specific for prostate cancer because t-PSA can be elevated due to factors other than prostate cancer. In particular, it is dangerous to confirm the diagnosis of prostate cancer when the t-PSA level falls in the diagnostic gray zone. Many studies showed that multiplexed detection of biomarkers is important for the clinical diagnostics of prostate cancer. In this work, we developed a SERS-based assay technique for the duplex detection of f-PSA and c-PSA in clinical serum. On the basis of our SERS-based assay results, we confirmed that simultaneous duplex detection of both PSA markers (f-PSA and c-PSA) can lead to more efficient and reliable *in vitro* diagnostics of prostate cancer than single marker (t-PSA) test. In addition, our duplex assay results for both PSA markers are consistent with the results previously reported by other assay methods.<sup>31,32</sup> Specially, we paid attention to the 13 clinical samples among the 30 samples in Table S1 for which the t-PSA level was in the gray zone. Figure 3 illustrates the SERS-based assay process for the simultaneous detection of f-PSA and c-PSA. Two different types of SERS nano tags, f-PSA antibody/MGITC-labeled Au NPs and c-PSA/XRITC-labeled AuNPs, were added to a microtube to form sandwich immunocomplexes on the surface of a magnetic bead. These magnetic immunocomplexes could be separated using a magnetic bar, and the Raman signals for each SERS nano tag were measured and analyzed for quantitative evaluation of both f-PSA and c-PSA in blood serum. Figure 5a displays Raman spectra for various concentrations of f-PSA and c-PSA spiked into human serum. Here, the concentration ranges of f-PSA and c-PSA were 5.0 pg/mL–50 ng/mL and 45.0 pg/mL–450 ng/mL, respectively. The Raman intensity of MGITC at 1614 cm<sup>-1</sup> concomitantly increased with the increase in f-PSA concentration. Similarly, as the c-PSA concentration increased, the Raman intensity of XRITC at 1614 cm<sup>-1</sup> also increased. On the

basis of these SERS-based assay results, the calibration curves for f-PSA and c-PSA were determined as shown in Figure 5b. These two calibration lines were used for quantitative estimation of both PSA markers in 13 clinical serum samples. The limits of detection (LODs) of f-PSA and c-PSA measured by this simultaneous SERS-based assay platform were estimated to be 0.012 ng/mL and 0.15 ng/mL, respectively. This assay platform has many advantages including low serum consumption (less than 10  $\mu$ L for each assay) and fast assay time (less than 1 h).

The free PSA to total-PSA (f/t) ratios for 13 clinical sera measured by ECL and SERS assays are compared in Table 1. The t-PSA levels in all samples were in the gray zone. It was previously reported that the likelihood of a positive biopsy is 8% if the percentage of free PSA is greater than 25% compared with a likelihood of 56% if the percentage of free PSA is less than 10%. As shown in Table 1, the f/t ratios measured from the SERS-based assay were consistent with those measured from the ECL system within the clinically acceptable range. As shown in this table, only two samples (#3 and #13) had abnormal cutoff values of less than 25% f/t PSA ratio in the ECL assay. In contrast, three samples had abnormal values for parallel (#1, #5, and #13) and simultaneous (#3, #4, and #13) SERS-based assays, respectively. Here, the f/t ratio value ranged from 0.26 to 0.31 for all samples except #13. Since the f/t ratios for #1, #3, #4, and #5 were not much greater than 0.25, integration of other biomarkers and clinical variables into the f/t PSA ratio model is expected to improve the predictive value of PSA and thus potentially reduce the rate of unnecessary biopsies. In addition, analytical precision was investigated by analyzing the % coefficient variations (CVs) for parallel and simultaneous assays. %CVs were calculated from 13 clinical samples with five replicates. As shown in Table S1, the %CVs were estimated to be 16.38 and 6.57 for parallel and simultaneous SERS-based assays, respectively. This means that precision for the f/t-PSA ratio measured by the simultaneous assay was clearly better than that measured by the parallel assay.

For validation of the proposed assay technique for 13 clinical samples, Passing–Boblok regression analyses between ECL and parallel SERS-based assay (Figure 6a) and between ECL and

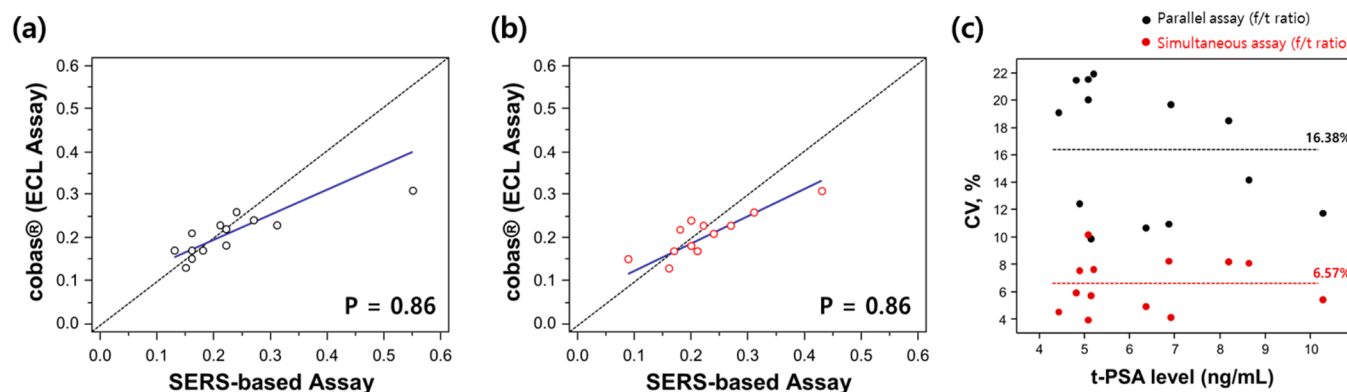


**Figure 6.** Passing–Boblok regression analyses (a) between ECL and parallel SERS-based assay and (b) between ECL and simultaneous SERS-based assay. (c) Distributions of the standard deviations for the CVs of parallel (black) and simultaneous (red) SERS-based assays for 13 clinical samples.

simultaneous SERS-based assay (Figure 6b) were performed. This is a statistical procedure that allows estimation of variation and systematic bias between two different analytical methods. If the 95% confidence intervals (CIs) for the slope and the intercept include 0 and 1, there is good conformity between two analytical methods. Since the scattered points (black) and regression lines (blue) of the data were included within the 95% CIs, it was concluded that all values were in the clinically acceptable range, and that the SERS-based assay data were valid for clinical samples in the gray zone. Figure 6c displays the distributions of the standard deviations for the CVs of parallel (black) and simultaneous (red) SERS-based assays in 13 clinical samples. The simultaneous assay data were characterized by a narrower distribution of standard deviations than the parallel assay data. Therefore, it was concluded that the assay result of *f/t* PSA ratios for 13 human sera in the gray zone measured by the simultaneous SERS-based assay showed better accuracy than those measured by the parallel SERS-based assay.

## CONCLUSION

Measurement of the free to total PSA ratio in clinical serum is known to improve the diagnostic performance for prostate cancer in patients with *t*-PSA antigen in the gray zone between 4.0 and 10.0 ng/mL. In the present study, a SERS-based immunoassay technique for the determination of free to total PSA ratio was developed. To assess the clinical feasibility of the proposed assay technique, the SERS-based *t*-PSA assay was performed for 30 clinical samples, and the assay results were compared with those measured by the ECL instrument installed in a clinical laboratory of University Hospital. The SERS-based assay results of *t*-PSA in 30 clinical sera showed a good linear relationship with those measured using the COBAS ECL system.

Additionally, parallel and simultaneous SERS-based assays for *f*-PSA and *c*-PSA were performed for 13 clinical samples in the gray zone for more reliable prostate cancer diagnostics. It is known that simultaneous assay for dual biomarkers provides a high detection throughput with low sample consumption compared with a parallel assay. The LODs for *f*-PSA and *c*-PSA were estimated to be 0.012 ng/mL and 0.15 ng/mL, respectively. In addition, a small volume of clinical serum (less than 10  $\mu$ L) and a short assay time (less than 1 h) are required for each assay process. According to our SERS-based assay results, the *f/t* PSA ratio measured by the simultaneous detection method also provides better precision since the

distributions of the standard deviations for %CVs were estimated to be much smaller than those measured by the parallel detection method. Therefore, the SERS-based assay for the simultaneous detection of dual PSA markers has strong potential as an innovative tool for accurate diagnosis of prostate cancer especially for clinical samples in the gray zone.

## EXPERIMENTAL METHODS

**Materials.** Gold(III) chloride trihydrate ( $\text{HAuCl}_4$ ), trisodium citrate ( $\text{Na}_3\text{-citrate}$ ), 1-ethyl-3-(3-dimethylamino)propyl) carbodiimide (EDC), *N*-hydroxysuccinimide (NHS), thiol-PEG-COOH (HS-PEG-COOH, MW  $\sim$ 3500), poly(ethylene glycol) methyl ether thiol (HS-PEG, MW 2000), phosphate-buffered saline (PBS) solution, and casein blocking agent were purchased from Sigma-Aldrich (St. Louis, MO, USA). Malachite green isothiocyanate (MGITC), X-rhodamine-5-(and-6)-isothiocyanate (XRITC), PBS buffer (10  $\times$ , pH 7.4), and carboxylic-activated magnetic beads (Dynabeads MyOne<sup>TM</sup>) were purchased from Invitrogen (Eugene, OR, USA). The free form of prostate-specific antigen protein (*f*-PSA),  $\alpha$ 1-antichymotrypsin-PSA protein (PSA/ACT), and mouse anti-PSA/ACT monoclonal antibody were purchased from Fitzgerald (Concord, MA, USA). Rabbit antitotal-PSA (*t*-PSA) polyclonal antibody was from Mybiosource, Inc. (San Diego, CA, USA). Mouse anti-*f*-PSA monoclonal antibody was purchased from Abcam (Cambridge, UK). Ultrapure water (18  $\text{M}\Omega\text{-cm}^{-1}$ ) was used in the experiments. All other reagents were of analytical reagent grade, and were used without further purification.

**Methods. Instrumentation.** High-magnification transmission electron microscopy (TEM) images were obtained using a JEOL TEM 2100F instrument (JEOL, Tokyo, Japan) at an accelerating voltage of 200 kV. Dynamic light scattering (DLS) data were acquired using a Nano-ZS90 (Malvern) apparatus (Malvern Instruments, Malvern, UK). UV/visible absorption spectra were measured with a Cary 100 spectrophotometer (Varian, Salt Lake City, UT, USA). Raman spectra were measured using an inVia Renishaw Raman microscope system (Renishaw, New Mills, UK). A Melles Griot He–Ne laser at 633 nm was used as the excitation source with power of 5 mW. The Rayleigh line was removed using an edge filter located in the collection path. Raman scattering signal was collected using a charge-coupled device (CCD) camera with a spectral resolution of 4  $\text{cm}^{-1}$ . PSA immunocomplexes in a microtube were transferred to a capillary tube, and their Raman scattering signals were measured by focusing a laser spot on the tube using a 20 $\times$  objective lens. Baseline correction of each Raman spectrum was performed using Renishaw WIRE 4.0 software. Polynomial algorithm (polynomial order = 11) was used to all points in each spectrum, and the baseline was corrected as zero.

**Preparation of SERS Nano Tags.** Au NPs were prepared according to the citration reduction method reported by Frens. First, 50 mL of 0.01%  $\text{HAuCl}_4$  solution was heated to the boiling point. Then, 0.5 mL of 1%  $\text{Na}_3\text{-citrate}$  solution was added to the boiling solution, and the

mixture solution was vigorously stirred. At this stage, the color of gold colloids changed to garnet red, indicating the formation of Au NPs. DLS and TEM measurements were performed to measure the size of Au NPs. Two different types of SERS nano tags were prepared for simultaneous detection of f-PSA and c-PSA. First, two Raman reporters, 4  $\mu\text{L}$  of  $10^{-5}$  M MGITC and 3  $\mu\text{L}$  of  $10^{-4}$  M XRITC, were respectively added to 1.0 mL of 0.12 nM Au NP solutions. After shaking for 10 min, 60  $\mu\text{L}$  of 10  $\mu\text{M}$  HS-PEG-COOH linker was added dropwise to MGITC- and XRITC-labeled Au NPs under vigorous stirring. After 30 min, 120  $\mu\text{L}$  of freshly prepared 10  $\mu\text{M}$  HS-PEG solution was added and reacted for 3 h. Before the antibody conjugation, PEGylated Au NPs were purified through three rounds of centrifugation (7200 rpm, 10 min) and redispersed in 10 mM PBS buffer solution (pH 7.2). The  $-\text{COOH}$  terminal groups on the surface of the AuNPs were activated by addition of 5  $\mu\text{L}$  of 25 mM EDC and 5  $\mu\text{L}$  of 25 mM NHS at 25  $^{\circ}\text{C}$ . Excess EDC and NHS were separated from the activated Au NPs through three rounds of centrifugation (7200 rpm, 10 min) and redispersed in 10 mM PBS buffer solution. The PEGylated AuNPs with activated carboxyl groups were then reacted with anti-f-PSA antibodies at 25  $^{\circ}\text{C}$  for 2 h, and the reaction mixture was stored at 4  $^{\circ}\text{C}$ . Excess antibodies were removed through three rounds of centrifugation (7200 rpm, 10 min) and resuspended in 10 mM PBS buffer solution (pH 7.4).

**Preparation of Total-PSA Antibody-Conjugated Magnetic Beads.** For conjugation of t-PSA antibodies on the surface of magnetic beads, 5  $\mu\text{L}$  of 0.1 M EDC and 5  $\mu\text{L}$  of 0.1 M NHS were added to 400  $\mu\text{L}$  of 0.5 mg/mL magnetic beads and allowed to react for 30 min with gentle mixing. After incubation, the beads were separated by a magnet and washed twice with 10 mM PBS buffer solution. The beads were resuspended in 0.5 mL of 10 mM PBS buffer and reacted with 13  $\mu\text{L}$  of 1 mg/mL anti-t-PSA antibodies for 2 h with continuous shaking (500 rpm) at room temperature. Unreacted antibodies were removed by washing three times out with 10 mM PBS buffer. Following addition of 20  $\mu\text{L}$  of 0.1% casein blocking buffer and incubation for 1 h at room temperature, unreacted  $-\text{COOH}$  groups were deactivated by incubation with 10  $\mu\text{L}$  of 3.0 mM ethanolamine for 2 h. The final product was stored in 10 mM PBS buffer at 4  $^{\circ}\text{C}$  for further use.

**Assays of Clinical Serum Samples.** To assess the clinical applicability and diagnostic capability of our proposed SERS-based immunoassay method, we performed the assays on clinical serum samples. A total of 30 clinical serum samples were collected from patients with prostate cancer at Korea University Hospital. This clinical study was approved by the Institutional Review Board (IRB) at the hospital. Consent documents were also obtained from all patients included in this study. All serum samples were stored at  $-80^{\circ}\text{C}$  until use. The concentrations of f-PSA and c-PSA for each of the 13 clinical serum samples were simultaneously determined using the proposed SERS-based dual marker assay protocol. Additionally, each clinical sample was assayed using a commercially available ECL assay system (ARCHITECT, Abbott Laboratories, USA) installed at Korea University Hospital. Finally, the SERS-based assay results were compared with those determined by the ECL assay protocol.

**Statistical Analysis of the Proposed Immunoassay.** To estimate the possible systematic bias and analytical agreement between the ECL assay and SERS-based assay, Passing–Bablok regression analyses were performed on clinical data using the MedCalc program (Ostend, Belgium).

## ASSOCIATED CONTENT

### Supporting Information

The Supporting Information is available free of charge on the ACS Publications website at DOI: 10.1021/acsnano.7b01536.

t-PSA concentration data determined by ECL- and SERS-based assays for 30 clinical samples; Raman spectra and corresponding calibration curve for 12 t-PSA spiked human serum samples; Passing–Bablok regression analyses of t-PSA for 30 clinical samples (PDF)

## AUTHOR INFORMATION

### Corresponding Authors

\*E-mail: lxchen@yic.ac.cn.

\*E-mail: jbachoo@hanyang.ac.kr.

### ORCID

Lingxin Chen: 0000-0002-3764-3515

Jaebum Choo: 0000-0003-3864-6459

### Notes

The authors declare no competing financial interest.

## ACKNOWLEDGMENTS

The National Research Foundation of Korea supported this work through grant numbers R11-2008-0061852 and K2090400004-12A0500-00410. The Nano Material Technology Development Program also supported this work, through the National Research Foundation of Korea, funded by the Ministry of Education, Science, and Technology (grant number 2012035286). This work was also partially supported by the Korea Health Industry Development Institute (KHIDI) funded by the Ministry of Health and Welfare, Korea (HI16C2129). L.C. thanks the National Natural Science Foundation of China (21575159) for financial support.

## REFERENCES

- (1) Bhindi, B.; Mamdani, M.; Kulkarni, G. S.; Finelli, A.; Hamilton, R. J.; Trachtenberg, J.; Zlotta, A. R.; Evans, A.; van der Kwast, T. H.; Toi, A.; Fleshner, N. E. Impact of the U.S. Preventive Services Task Force Recommendations against Prostate-Specific Antigen Screening on Prostate Biopsy and Cancer Detection Rates. *J. Urol.* **2015**, *193*, 1519–1524.
- (2) Stephan, C.; Köpke, T.; Semjonow, A.; Lein, M.; Deger, S.; Schrader, M.; Miller, K.; Jung, K. Discordant Total and Free Prostate-Specific Antigen (PSA) Assays: Does Calibration with WHO Reference Materials Diminish the Problem? *Clin. Chem. Lab. Med.* **2009**, *47*, 1325–1331.
- (3) Kim, E. H.; Andriole, G. L. Prostate-Specific Antigen-Based Screening: Controversy and Guidelines. *BMC Med.* **2015**, *13*, 61–64.
- (4) Cooperberg, M. R.; Lubeck, D. P.; Meng, M. V.; Mehta, S. S.; Carroll, P. R. The Changing Face of Low-Risk Prostate Cancer: Trends in Clinical Presentation and Primary Management. *J. Clin. Oncol.* **2004**, *22*, 2141–2149.
- (5) Zhu, L.; Leinonen, J.; Zhang, W. M.; Finne, P.; Srenman, U. H. Dual-Label Immunoassay for Simultaneous Measurement of Prostate-Specific Antigen (PSA)- $\alpha_1$ -Antichymotrypsin Complex Together with Free or Total PSA. *Clin. Chem.* **2003**, *49*, 97–103.
- (6) Jung, K.; Elgeti, U.; Lein, M.; Brux, B.; Shinha, P.; Rudolph, B.; Hauptmann, S.; Schnorr, D.; Loening, S. A. Ratio of Free or Complexed Prostate-Specific Antigen (PSA) to Total PSA: Which Ratio Improves Differentiation between Benign Prostatic Hyperplasia and Prostate Cancer. *Clin. Chem.* **2000**, *46*, 55–62.
- (7) Catalona, W. J.; Partin, A. W.; Slawin, K. M.; Brawer, M. K.; Flanigan, R. C.; Patel, A.; Richie, J. P.; deKernion, J. B.; Walsh, P. C.; Scardino, P. T.; Lange, P. H.; Subong, E. N. P.; Parson, R. E.; Gasior, G. H.; Loveland, K. G.; Southwick, P. C. Use of the Percentage of Free Prostate-Specific Antigen to Enhance Differentiation of Prostate Cancer from Benign Prostatic Disease. *JAMA* **1998**, *279*, 1542–1547.
- (8) Luderer, A. A.; Chen, Y. T.; Soriano, T. F.; Kramp, W. J.; Carlson, G.; Cuny, C.; Sharp, T.; Smith, W.; Petteway, J.; Brawer, M.; Thiel, R. Measurement of the Proportion of Free to Total Prostate-Specific Antigen Improves Diagnostic Performance of Prostate-Specific Antigen in the Diagnostic Gray Zone of Total Prostate-Specific Antigen. *Urology* **1995**, *46*, 187–194.
- (9) Stephan, C.; Klaas, M.; Muller, C.; Schnorr, D.; Loening, S. A.; Jung, K. Interchangeability of Measurements of Total and Free

Prostate-Specific Antigen in Serum with 5 Frequently Used Assay Combinations: an Update. *Clin. Chem.* **2006**, *52*, 59–64.

(10) Slev, P. R.; La'ulu, S. L.; Roberts, W. L. Intermethod Differences in Results for Total PSA, Free PSA, and Percentage of Free PSA. *Am. J. Clin. Pathol.* **2008**, *129*, 952–958.

(11) Liang, J.; Liu, H.; Huang, C.; Yao, C.; Fu, Q.; Li, X.; Cao, D.; Luo, Z.; Tang, Y. Aggregated Silver Nanoparticles Based Surface-Enhanced Raman Scattering Enzyme-Linked Immunosorbent Assay for Ultrasensitive Detection of Protein Biomarkers and Small Molecules. *Anal. Chem.* **2015**, *87*, 5790–5796.

(12) Li, X.; Li, W.; Yang, Q.; Gong, X.; Guo, W.; Dong, C.; Liu, J.; Xuan, L.; Chang, J. Rapid and Quantitative Detection of Prostate Specific Antigen with a Quantum Dot Nanobeads-Based Immunochromatography Test Strip. *ACS Appl. Mater. Interfaces* **2014**, *6*, 6406–6414.

(13) Jiang, Z.; Qin, Y.; Peng, Z.; Chen, S.; Chen, S.; Deng, C.; Xiang, J. The Simultaneous Detection of Free and Total Prostate Antigen in Serum Samples with High Sensitivity and Specificity by Using the Dual-Channel Surface Plasmon Resonance. *Biosens. Bioelectron.* **2014**, *62*, 268–273.

(14) Spain, E.; Gilgunn, S.; Sharma, S.; Adamson, K.; Carthy, E.; O'Kennedy, R.; Forster, R. J. Detection of Prostate Specific Antigen Based on Electrocatalytic Platinum Nanoparticles Conjugated to a Recombinant scFv Antibody. *Biosens. Bioelectron.* **2016**, *77*, 759–766.

(15) Poon, C. Y.; Chan, H. M.; Li, H. W. Direct Detection of Prostate Specific Antigen by Darkfield Microscopy Using Single Immunotargeting Silver Nanoparticle. *Sens. Actuators, B* **2014**, *190*, 737–744.

(16) Liu, A.; Zhao, F.; Zhao, Y.; Shanguan, L.; Liu, S. A Portable Chemiluminescence Imaging Immunoassay for Simultaneous Detection of Different Isoforms of Prostate Specific Antigen in Serum. *Biosens. Bioelectron.* **2016**, *81*, 97–102.

(17) Liu, X.; Dai, Q.; Austin, L.; Coutts, J.; Knowles, G.; Zou, J.; Chen, H.; Huo, Q. A One-Step Homogeneous Immunoassay for Cancer Biomarker Detection Using Gold Nanoparticle Probes Coupled with Dynamic Light Scattering. *J. Am. Chem. Soc.* **2008**, *130*, 2780–2782.

(18) Tang, B.; Wang, J.; Hutchison, J. A.; Ma, L.; Zhang, N.; Guo, H.; Hu, Z.; Li, M.; Zhao, Y. Ultrasensitive, Multiplex Raman Frequency Shift Immunoassay of Liver Cancer Biomarkers in Physiological Media. *ACS Nano* **2016**, *10*, 871–879.

(19) Porter, M. D.; Lipert, R. J.; Siperko, N. M.; Wang, G.; Narayanan, R. SERS As a Bioassay Platform: Fundamentals, Design, and Applications. *Chem. Soc. Rev.* **2008**, *37*, 1001–1011.

(20) Li, M.; Cushing, S. K.; Zhang, J.; Suri, S.; Evans, R.; Petros, W. P.; Gibson, L. F.; Ma, D.; Liu, Y.; Wu, N. Three-Dimensional Hierarchical Plasmonic Nano-Architecture Enhanced Surface-Enhanced Raman Scattering Immunosensor for Cancer Biomarker Detection in Blood Plasma. *ACS Nano* **2013**, *7*, 4967–4976.

(21) Chon, H.; Lee, S.; Yoon, S. Y.; Lee, E. K.; Chang, S. I.; Choo, J. SERS-Based Competitive Immunoassay of Troponin I and CK-MB Markers for Early Diagnosis of Acute Myocardial Infarction. *Chem. Commun.* **2014**, *50*, 1058–1060.

(22) Ye, J.; Chen, Y.; Liu, Z. A Boronate Affinity Sandwich Assay: An Appealing Alternative to Immunoassays for the Determination of Glycoproteins. *Angew. Chem., Int. Ed.* **2014**, *53*, 10386–10389.

(23) Wang, Y.; Vaidyanathan, R.; Shiddiky, M. J. A.; Trau, M. Enabling Rapid and Specific Surface-Enhanced Raman Scattering Immunoassay Using Nanoscaled Surface Shear Forces. *ACS Nano* **2015**, *9*, 6354–6362.

(24) Nie, S.; Emory, S. R. Probing Single Molecules and Single Nanoparticles by Surface-Enhanced Raman Scattering. *Science* **1997**, *275*, 1102–1106.

(25) Harper, M. M.; McKeating, K. S.; Faulds, K. Recent Development and Future Directions in SERS for Bioanalysis. *Phys. Chem. Chem. Phys.* **2013**, *15*, 5312–5328.

(26) Wang, R.; Chon, H.; Lee, S.; Cheng, Z.; Hong, S. H.; Yoon, Y.; Choo, J. Highly Sensitive Detection of Hormone Estradiol E2 Using Surface-Enhanced Raman Scattering Based Immunoassays for the

Clinical Diagnosis of Precocious Puberty. *ACS Appl. Mater. Interfaces* **2016**, *8*, 10665–10672.

(27) Guerrini, L.; Pazos, E.; Penas, C.; Vazquez, M. E.; Mascarenas, J. L.; Alvarez-Puebla, R. A. Highly Sensitive SERS Quantification of the Oncogenic Protein c-Jun in Cellular Extracts. *J. Am. Chem. Soc.* **2013**, *135*, 10314–10317.

(28) Hwang, J.; Lee, S.; Choo, J. Application of a SERS-Based Lateral Flow Immunoassay Strip for the Rapid and Sensitive Detection of Staphylococcal Enterotoxin B. *Nanoscale* **2016**, *8*, 11418–11425.

(29) Chon, H.; Lee, S.; Yoon, S. Y.; Chang, S. I.; Lim, D. W.; Choo, J. Simultaneous Immunoassay for the Detection of Two Lung Cancer Markers Using Functionalized SERS Nanoprobles. *Chem. Commun.* **2011**, *47*, 12515–12517.

(30) Lee, S.; Chon, H.; Yoon, S. Y.; Lee, E. K.; Chang, S. I.; Lim, D. W.; Choo, J. Fabrication of SERS-Fluorescence Dual Modal Nanoprobles and Application to Multiplex Cancer Cell Imaging. *Nanoscale* **2012**, *4*, 124–129.

(31) Zheng, G.; Patolsky, F.; Cui, Y.; Wang, W. U.; Lieber, C. M. Multiplexed Electrical Detection of Cancer Markers with Nanowire Sensor Arrays. *Nat. Biotechnol.* **2005**, *23*, 1294–1301.

(32) Kingsmore, S. F. Multiplexed Protein Measurement: Technologies and Applications of Protein and Antibody Arrays. *Nat. Rev. Drug Discovery* **2006**, *5*, 310–321.